

Neuron, Volume 100

Supplemental Information

**Precise Synaptic Balance
in the Zebrafish Homolog of Olfactory Cortex**

Peter Rupprecht and Rainer W. Friedrich

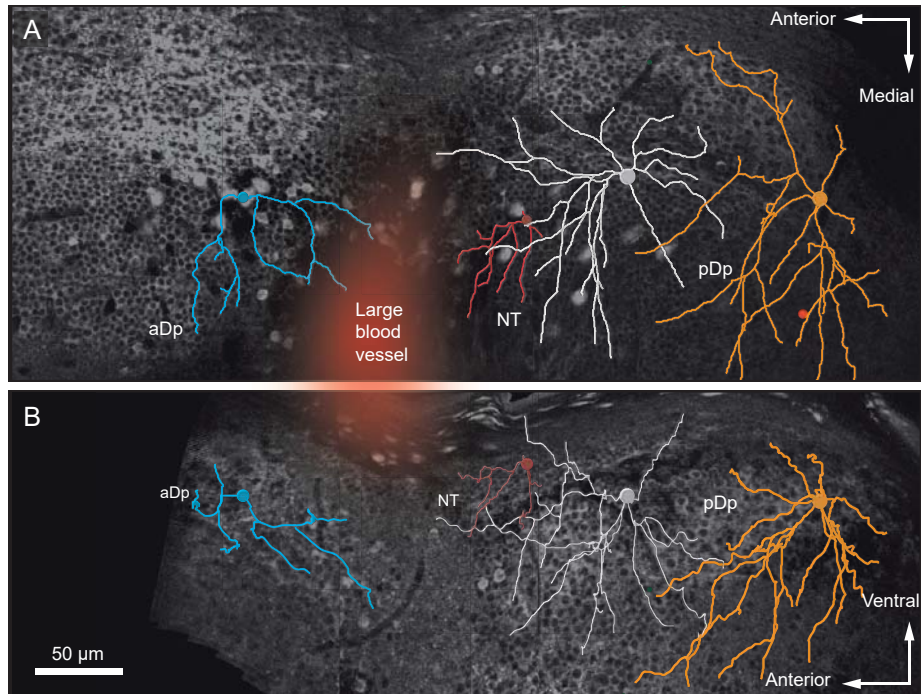


Figure S1. Morphology of neurons in Dp. Related to Fig. 1. Examples of reconstructed neurons in aDp (blue), NT (red) and pDp (white, yellow) in horizontal (A) and sagittal (B) surface projections of the reference brain. Additional examples are shown in Movie S1.

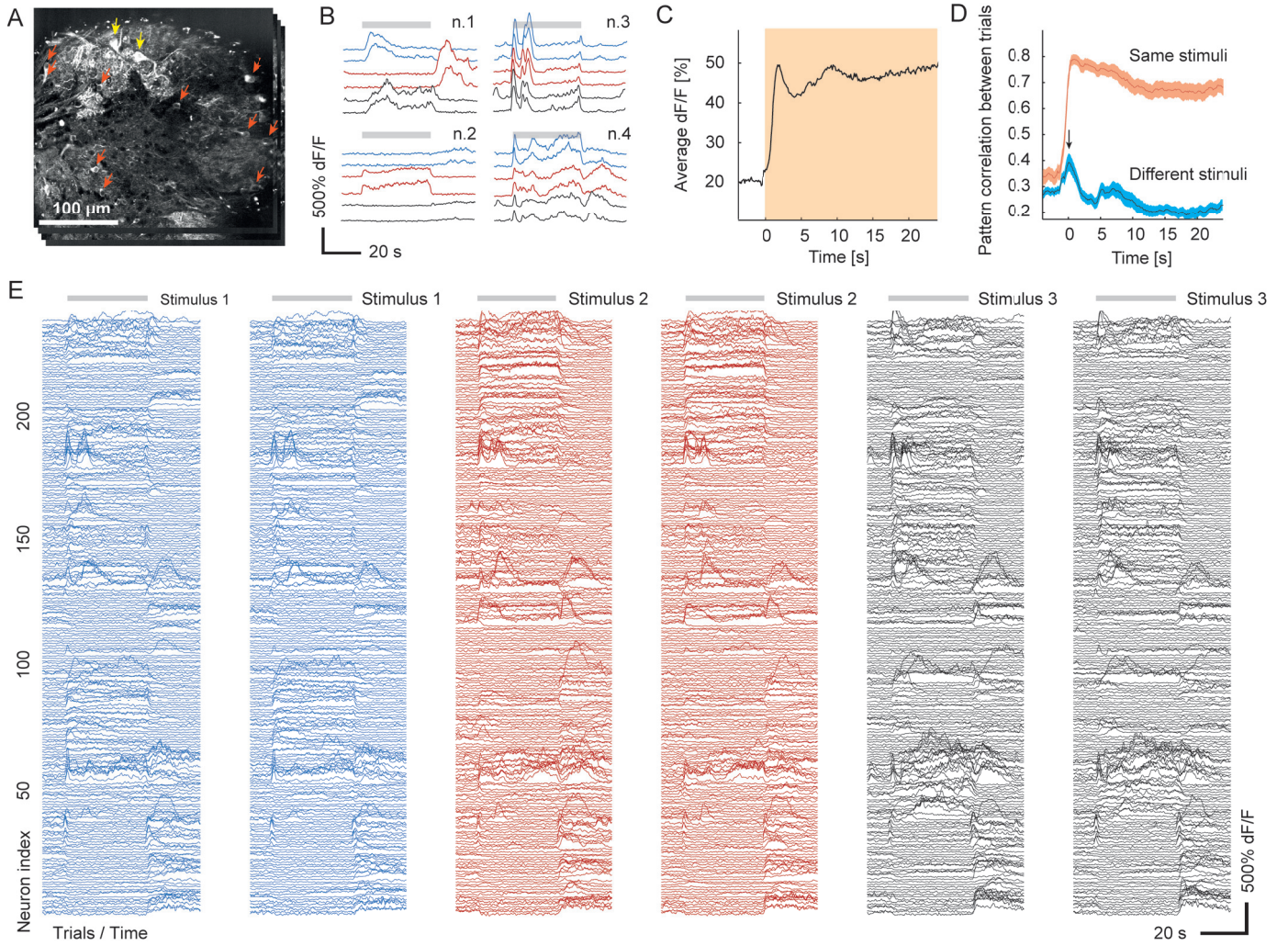


Figure S2. Activity patterns across mitral cells in the OB. Related to Fig. 2. **A.** Raw fluorescence in one of four simultaneously recorded optical sections through the OB of a fish expressing GCaMP5 in mitral cells (HuC-GCaMP5; (Ahrens et al., 2013)). Mitral cells (arrows) are distinguished from interneurons by their large somata and characteristic dendritic tufts. Yellow arrows depict mitral cells with dendritic tufts in the same image plane; red arrows depict additional mitral cells with dendritic tufts in other planes (not shown). **B.** Time course of responses ($\Delta F/F$) of four mitral cells to three different odors, two repetitions each. Odor stimulation (35 s) is indicated by gray bar. **C.** Response ($\Delta F/F$) averaged over all neurons ($n_{\text{neurons}} = 424$ from 10 fish), odors ($n_{\text{odors}} = 3$) and trials ($n_{\text{trials}} = 2$). Odors were [Ala, Arg, Phe] in 302 neurons and [Ala, His, Trp] in 122 neurons. **D.** Correlation of activity patterns across mitral cells between trials as a function of time, averaged across fish. Red: same odor stimulus; blue: different odors. Color bands show s.e.m.. Arrow depicts initial correlation that decreases subsequently. **E.** Responses ($\Delta F/F$) of mitral cells that responded strongly to at least one of the three stimuli ($n = 250$; three odors, two repetitions each). Stimulus identity ([Ala, Arg, Phe] or [Ala, His, Trp]) is color-coded. The onset of odor responses was determined by the rise of the baseline-subtracted average to 10% of the maximum.

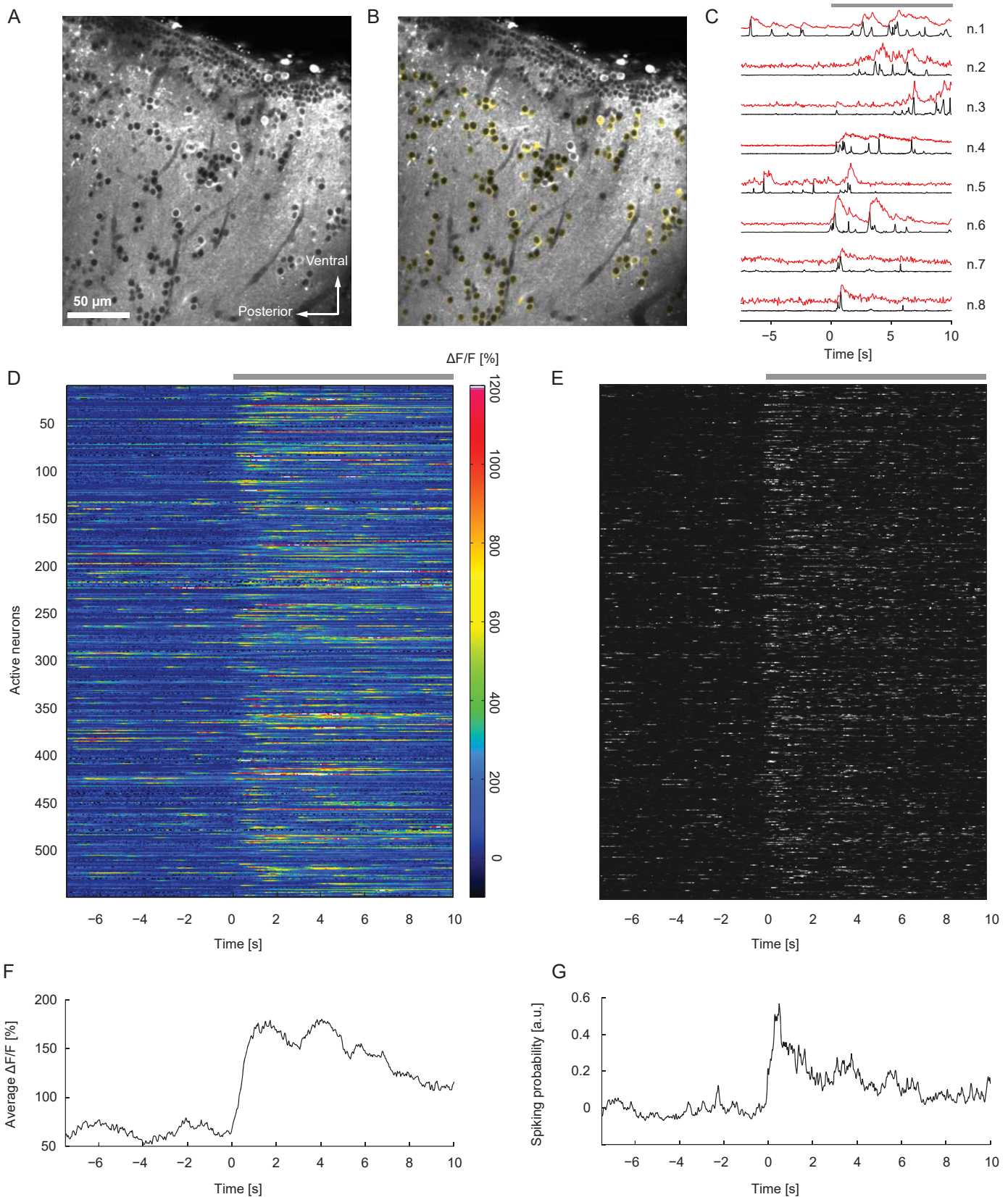


Figure S3. Odor-evoked activity in pDp. Related to Fig. 2. **A.** Sagittal optical section through pDp. **B.** Regions of interest corresponding to neuronal somata in pDp (yellow) overlaid on the same optical section. Small somata at the top of the image are NT neurons (not marked). **C.** Red: calcium signals ($\Delta F/F$) of eight Dp neurons during odor stimulation (grey bar). Black: spiking probability (firing rate) estimated from calcium signals by an algorithm based on machine learning (Berens et al., 2018). **D.** Calcium signals ($\Delta F/F$) of all neurons that were active during the recording period (545 of 3'848 recorded neurons). A total of 15 trials were recorded in 6 fish (11x food stimulus, 3x tryptophan, 1x arginine). All traces show single trials. **E.** Spiking probabilities reconstructed from calcium signals in (D) (arbitrary scaling). **F.** Average across all $\Delta F/F$ traces in (D). **G.** Average across traces in (E). The response onset was selected manually based on a plot of average, median and top 95 percentile $\Delta F/F$ activity across all active neurons for each trial. The manually selected onset $\Delta F/F$ value corresponded to approximately 10 - 15% of the maximum response.

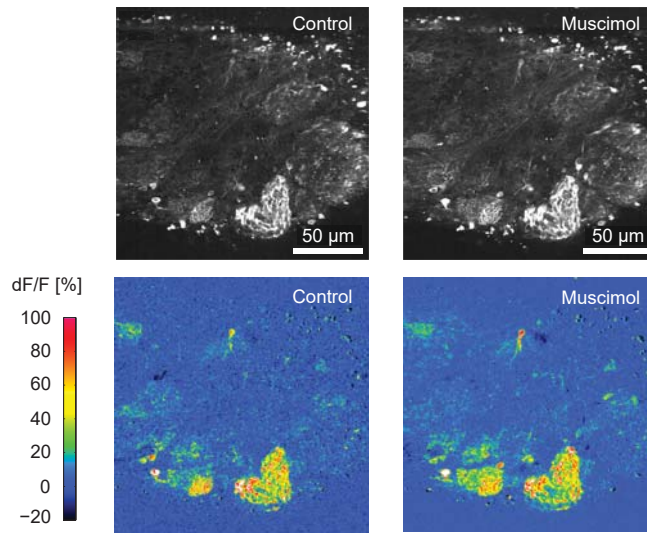


Figure S4. Effects of muscimol on odor-evoked activity in the OB. Related to Fig. 3. Raw fluorescence in an optical section through the OB (top) and change in stimulus-evoked fluorescence ($\Delta F/F$, food stimulus, bottom). Left: before injection of muscimol; right: after muscimol injection into Dp (individual trials; time between odor applications $\Delta t \sim 30$ min).

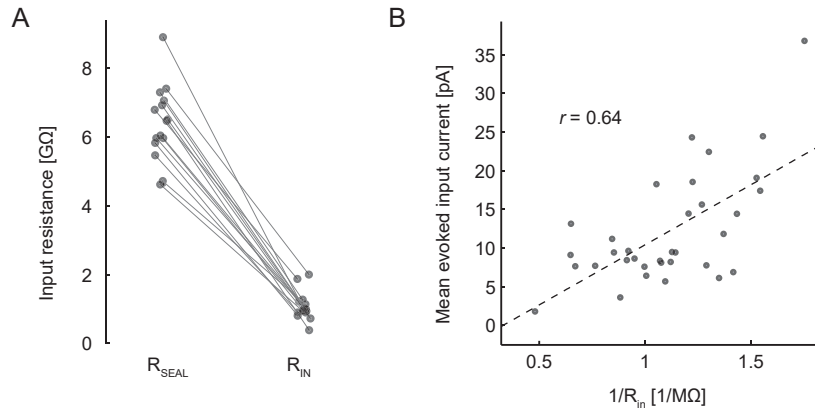


Figure S5. Related to Figs. 4 and 6. **A.** Membrane resistance error due to seal resistance and break-in. Resistances measured before (R_{seal}) and after break-in (R_{in}) in pDp ($n = 15$ neurons). The seal resistance R_{seal} was, on average, approximately 6-fold higher than the measured input resistances R_{in} . As a consequence, resting conductances were overestimated by approximately 25% and odor-evoked conductance changes were underestimated by approximately 25%. Measurements were not corrected for this factor. **B.** Correlation between inverse input resistance and odor-evoked input current in pDp neurons. The mean odor-evoked input current of each pDp neuron was determined by averaging both over the first 1.5 seconds after response onset and over all available trials and over EPSCs and IPSCs (absolute values). The correlation between the inverse input resistance $1/R_{in}$ and the mean odor-evoked input current was $r = 0.64$ ($p = 4.6e-5$; $n = 34$ neurons). Dashed line: linear fit.

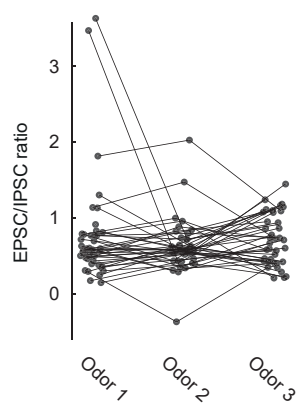


Figure S6. Related to Fig. 4. Ratio of excitatory and inhibitory currents, averaged over the first 1.5 s after the odor response onset for all neuron-odor pairs. Data points from the same neurons are connected by lines.

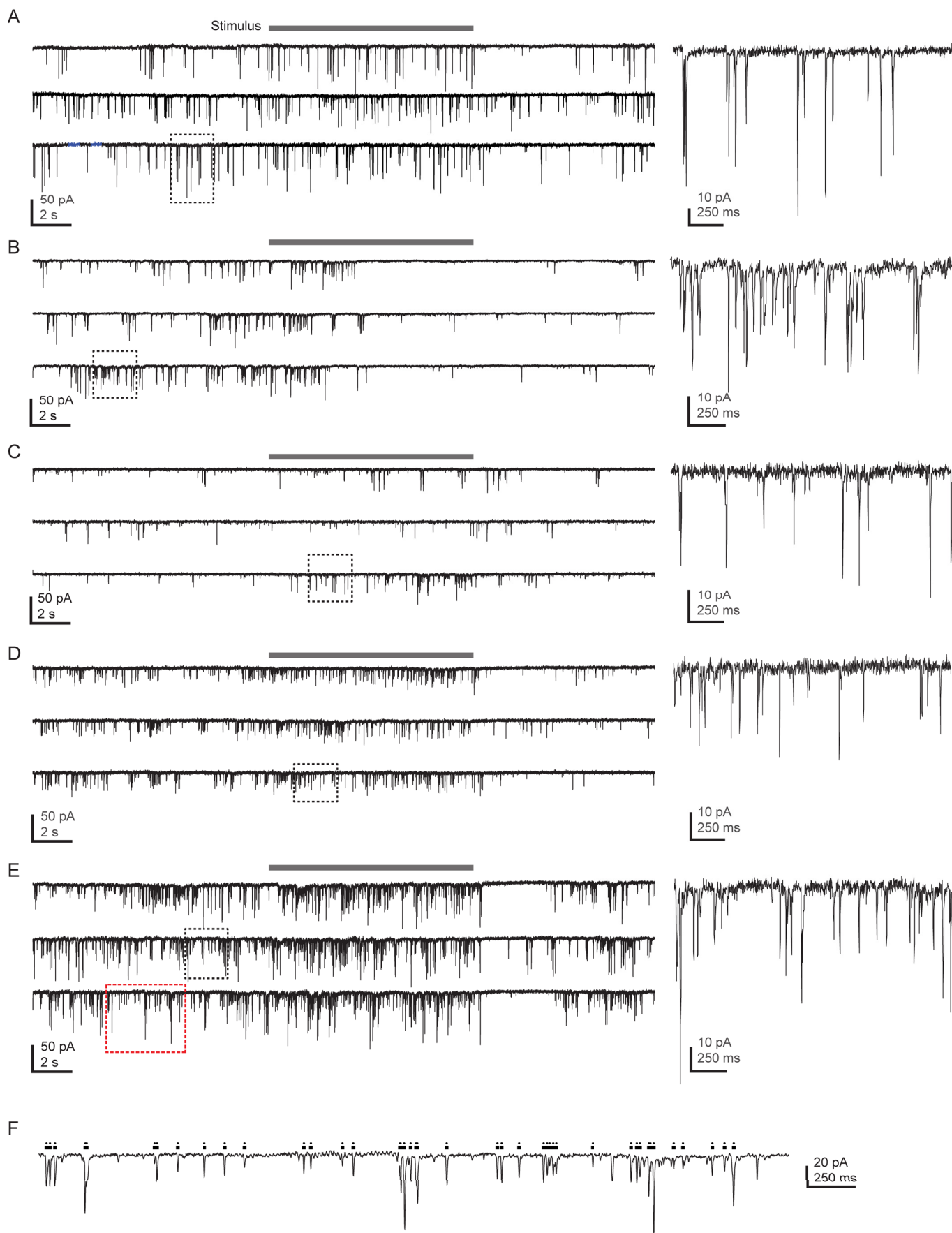


Figure S7. Examples of EPSCs in aDp neurons and EPSC event detection. Related to Fig. 5. **A-E.** Example EPSCs in five different aDp neurons (three repetitions of a single stimulus: arginine, histidine, food extract, TDCA, food extract). The dotted black rectangle highlights a 2 s window that is enlarged on the right. Note large and discrete events occurring at low frequency. Odor application is indicated by the black bar. **F.** Automated detection of excitatory events in whole-cell voltage clamp recordings from neurons in aDp. Example is taken from the time window outlined by the red rectangle in (E). Detected events are indicated by dots.